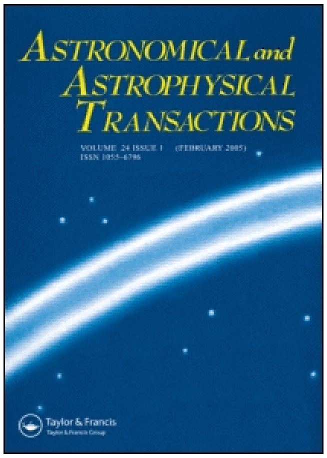

Astronomical & Astrophysical Transactions
The Journal of the Eurasian Astronomical Society
Publication details, including instructions for authors and subscription information:
http://www.informaworld.com/smpp/title~content=t713453505

Long-term starspot activity of the eclipsing binary **SV Cam**

G. Djurašević [a]
[a] Astronomical Observatory, Belgrade, Yugoslavia

Online Publication Date: 01 December 1999
To cite this Article: Djurašević, G. (1999) 'Long-term starspot activity of the eclipsing binary **SV Cam**', Astronomical & Astrophysical Transactions, 18:3, 499 - 507
To link to this article: DOI: 10.1080/10556799908203007
URL: http://dx.doi.org/10.1080/10556799908203007

Astronomical and Astrophysical Transactions, 1999, Vol. 18, pp. 499–507
Reprints available directly from the publisher
Photocopying permitted by license only

LONG-TERM STARSPOT ACTIVITY OF THE ECLIPSING BINARY *SV CAM*

G. DJURAŠEVIĆ

Astronomical Observatory, Belgrade, Yugoslavia

(Received November 30, 1997)

The paper is devoted to the problem of the determination of the orbital and physical parameters of the active eclipsing binary *SV Cam* on the basis of the interpretation of photometric observations made by Patkós (1982) during the period 1973–1981. The problem is solved in two stages: by obtaining a synthetic light curve in the case when the parameters of the corresponding Roche model (Djurašević, 1992a) are given *a priori* (direct problem), and by determining the parameters of the model for which the best fit between the synthetic light curve and the observations is achieved (inverse problem) (Djurašević, 1992b). A total of 18 light curves are analysed in the framework of the Roche model, involving two spotted regions on the primary component of the system (Sp G3 V), with the temperature contrast between the spotted area and the surrounding photosphere $A_s = T_s/T_1 = 0.65$. The basic parameters of the system and of the spotted areas are estimated. According to the obtained results the spotted areas are formed at high latitudes and cover a significant part of the stellar surface. No clear cyclicity of the system's activity is noted from the analysed observations. There are some indications that the spotted area at high latitudes (above 70°) corresponds to an enhanced activity. Since the system's period is short ($P \sim 0\overset{d}{.}59$), the presence of spotted regions at high latitudes can be explained by the dynamo mechanism for rapid rotators (Schüssler and Solanski, 1992). During the analysed period the spotted areas tend to fall into the specially active longitude sectors at high latitudes, near stellar polar regions. The light curve analysis allowed an estimation of the system's parameters and those of the active spotted regions.

KEY WORDS Eclipsing variable stars, orbital parameters, SV Cam

1 INTRODUCTION

The close binary (CB) *SV Cam* has the orbital period $P = 0\overset{d}{.}59307$. According to Hall (1976), it belongs to the short-period group of the *RS CVn* binaries. Hilditch *et al.* (1979) found that this system is composed of a G3V primary, and K4V secondary, with the mass ratio $q = m_2/m_1 = 0.7$. They made the hypothesis that the light variations are due to a *BY Draconis*-type variability of the K4V secondary. The careful photometry by Patkós (1982) proved conclusively the existence of a "distortion wave", which migrates toward increasing orbital phase, and strong flaring activity, which Patkós (1981) attributed to the active regions on the secondary star.

Observations extending over about half a century (1932–1984) were analysed by Zeilik *et al.* (1988) in the framework of the spot modelling technique (Budding, 1977; Budding and Zeilik, 1987) with spots on the primary. According to these authors, the active dark spotted region covers a significant part of the stellar surface occupying high latitudes ($\sim 60°$–$75°$). The single active region tends to fall into two longitude sectors, 45°–135° and 225°–315°. These resemble the *active longitude belts* such as those proposed by Eaton and Hall (1979) for the *RS CVn* group in general.

2 LIGHT CURVE ANALYSIS

The paper presents the analysis of the light curves of *SV Cam* observed in the period 1973–1981 (Patkós, 1982), which is based on the Roche model with spotted areas on the components (Djurašević, 1992a). For a successful application of the model in analysing the observed light curves an efficient method unifying the best properties of the steepest descent and the differential corrections methods into a single algorithm (Djurašević, 1992b) is proposed. This method is obtained by modifying Marquardt's (1963) algorithm.

The interpretation of photometric observations is based on the choice of optimal model parameters yielding the best agreement between the observed light curve and the corresponding synthetic one. Some of these parameters can be determined *a priori* in an independent way, while the others are found by solving the inverse problem. We obtained the optimal model parameters through the minimization of $S = \Sigma(O - C)^2$, where $O - C$ is the residual between observed (LCO) and synthetic (LCC) light curves for a given orbital phase. The minimisation of S is done in an iterative cycle of corrections of the model parameters.

Out of a total of 38 light curves, 18 (which are relatively well defined) are chosen to enable the estimate of the system's and spotted areas' parameters. In Table 1 the data sequence of the individual light curves is presented.

Since the critical Roche lobes are filled by the components to a high degree, tidal effects are expected to contribute to synchronization of the rotational and orbital periods. Therefore, in solving the inverse problem, we adopted the values $f_{1,2} = 1.0$ for non-synchronous rotation coefficients. The mass ratio is fixed by assuming the value $q = m_2/m_1 = 0.71$, estimated spectroscopically (Budding and Zeilik, 1987). Based on the primary's spectral type (G3V) its temperature is also fixed ($T_1 = 5800$ K).

In the programme for solving the inverse problem, the linear limb-darkening coefficients are determined from the stellar effective temperature and the stellar-surface gravity, according to the given spectral type, by using the polynomial proposed by Díaz-Cordovés *et al.* (1995). For the gravity-darkening coefficients of the stars the value of $\beta_{1,2} = 0.08$ was adopted. Lucy (1967) and Osaki (1970) regard this value as justifiable for stars with convective envelopes.

Table 1. Data sources for the analysis of the observed light curves (Patkós, 1982) for the active CB *SV Cam* (V-filter)

No	*Date*	*J.D.*	*N*
1	1973 Jan 04–1973 Jan 12	2441695, 2441696	98
2	1973 May 04–1973 Jun 02	2441807, 2441810, 2441824, 2441825, 2441831, 2441833, 2441835	107
3	1973 Aug 05–1973 Aug 11	2441900, 2441901, 2441903, 2441904, 2441905	97
4	1973 Oct 03–1973 Oct 06	2441959, 2441960, 2441961	135
5	1973 Oct 06–1973 Oct 08	2441962, 2441963	97
6	1973 Oct 26–1973 Oct 27	2441982	79
7	1973 Oct 27–1973 Oct 29	2441983, 2441984	138
8	1973 Dec 02–1973 Dec 03	2442019	98
9	1974 Feb 27–1974 Mar 02	2442106,2442108	71
10	1974 Dec 22–1974 Dec 24	2442404, 2442405	123
11	1975 Feb 16–1975 Feb 18	2442432, 2442460, 2442461	101
12	1975 Feb 21–1975 Feb 23	2442465, 2442466	87
13	1975 Apr 19–1975 Apr 21	2442522, 2442523	55
14	1976 Feb 20–1976 Feb 28	2442829, 2442830,2442831, 2442836	72
15	1977 Sep 05–1977 Sep 08	2443392, 2443393, 2443394	60
16	1979 Jan 04–1979 Jan 07	2443878, 2443879, 2443880	158
17	1980 Feb 15–1980 Feb 16	2444285	177
18	1980 Dec 08–1980 Dec 09	2444582	258

Note. No; data set number; J.D., Julian dates of the observations; N, total number of observations for the given light curve.

The temperature of the secondary ($T_2 \sim 4300$ K) was significantly lower than that of the primary. Therefore, its contribution to the total brightness of the system is relatively small. Therefore one can expect that the spotted areas on the secondary yield comparatively small photometric effects.

Under the assumption of spotted areas being on the primary, the optimum synthetic light curves fit the observations much better. For the temperature contrast between the spotted area and the surrounding photosphere it is assumed that $A_s = T_s/T_1 = 0.65$, yielding the spot temperature to be ~ 3770 K.

In analysing the light curves the following procedure is applied. First, on the basis of the light curve form, the curve No. 10 (see Tables 1–2 and Figure 2) was chosen as the cleanest of the spot effects. In its analysis, the optimisation begins using only the basic model parameters. After achieving the first convergence, one includes also free parameters related to spots in the iterative optimization process.

The basic parameters of the system, obtained in this way, are used as starting points in the inverse-problem solution for other light curves. Their analysis begins by optimization of the spot parameters. When the optimization based on these parameters does not provide a further minimization of $\Sigma(O - C)^2$, the system's basic parameters have to be introduced into the iterative process. Using this procedure we optimize all free-parameters of the model in the final iterations.

Table 2. Results of the analysis of the *SV Cam* light curves obtained by solving the inverse problem for the Roche model with two spotted areas on the primary component

No	θ_1	λ_1	φ_1	θ_2	λ_2	φ_2	F_1	F_2
1	50.7 ± 2.2	111 ± 7	86 ± 12	18.4 ± 0.9	303 ± 5	-53 ± 3	0.881 ± 0.006	0.641 ± 0.004
2	27.4 ± 0.4	60 ± 2	59 ± 1	14.9 ± 0.4	285 ± 2	-4 ± 3	0.885 ± 0.005	0.651 ± 0.003
3	44.8 ± 0.6	90 ± 2	70 ± 1	13.8 ± 0.7	285 ± 5	-7 ± 20	0.893 ± 0.006	0.638 ± 0.005
4	33.1 ± 0.2	109 ± 1	64 ± 1	12.3 ± 0.3	240 ± 3	-25 ± 3	0.897 ± 0.002	0.640 ± 0.002
5	41.2 ± 0.4	104 ± 2	71 ± 1	14.9 ± 0.4	242 ± 3	-30 ± 5	0.888 ± 0.003	0.632 ± 0.002
6	46.7 ± 1.1	201 ± 4	83 ± 1	15.5 ± 1.0	99 ± 3	-25 ± 13	0.888 ± 0.003	0.634 ± 0.002
7	34.6 ± 0.6	186 ± 2	72 ± 1	14.6 ± 0.4	78 ± 4	-58 ± 2	0.877 ± 0.003	0.633 ± 0.002
8	37.2 ± 0.5	241 ± 2	68 ± 1	12.8 ± 0.3	63 ± 2	-13 ± 4	0.886 ± 0.003	0.646 ± 0.002
9	37.9 ± 0.6	281 ± 3	63 ± 1	9.1 ± 1.0	112 ± 6	-22 ± 25	0.870 ± 0.008	0.640 ± 0.005
10	22.4 ± 0.5	245 ± 5	71 ± 1	7.5 ± 0.3	87 ± 7	-24 ± 5	0.871 ± 0.003	0.652 ± 0.002
11	30.2 ± 0.4	45 ± 1	66 ± 1	28.2 ± 0.3	275 ± 2	-60 ± 1	0.879 ± 0.003	0.642 ± 0.002
12	30.2 ± 0.4	45 ± 1	66 ± 1	27.4 ± 0.3	283 ± 2	-58 ± 1	0.876 ± 0.003	0.640 ± 0.002
13	52.9 ± 1.1	61 ± 4	86 ± 1	15.9 ± 0.4	269 ± 2	-17 ± 3	0.870 ± 0.003	0.635 ± 0.002
14	23.3 ± 6.9	206 ± 15	53 ± 35	22.8 ± 1.3	73 ± 8	-62 ± 3	0.884 ± 0.006	0.664 ± 0.004
15	31.8 ± 2.1	3 ± 21	83 ± 2	21.8 ± 0.6	65 ± 2	-52 ± 3	0.870 ± 0.007	0.647 ± 0.006
16	31.3 ± 0.8	233 ± 4	64 ± 1	16.5 ± 0.5	21 ± 2	-10 ± 6	0.862 ± 0.008	0.653 ± 0.006
17	33.2 ± 1.1	231 ± 3	82 ± 1	22.0 ± 0.3	78 ± 2	-61 ± 1	0.875 ± 0.006	0.644 ± 0.002
18	34.3 ± 0.4	318 ± 1	69 ± 1	31.1 ± 0.4	74 ± 2	-71 ± 1	0.874 ± 0.002	0.627 ± 0.001

No	T_2	i	u_2	Ω_1	Ω_2	R_1	R_2	$\Sigma(O-C)^2$
1	4390 ± 50	89.4 ± 0.7	0.76	3.623	4.404	0.339	0.210	0.02400
2	4300 ± 50	89.0 ± 0.6	0.76	3.607	4.450	0.341	0.213	0.01575
3	4390 ± 50	89.6 ± 0.9	0.76	3.583	4.516	0.344	0.209	0.02531
4	4380 ± 20	89.4 ± 0.2	0.76	3.567	4.508	0.345	0.210	0.00801
5	4330 ± 30	89.9 ± 0.4	0.76	3.599	4.552	0.342	0.207	0.00928
6	4340 ± 20	89.4 ± 0.9	0.76	3.596	4.540	0.342	0.218	0.00371
7	4220 ± 30	89.7 ± 0.6	0.77	3.634	4.546	0.338	0.207	0.01008
8	4220 ± 30	89.4 ± 0.6	0.77	3.606	4.474	0.341	0.212	0.00626
9	4250 ± 80	89.5 ± 0.7	0.77	3.660	4.508	0.335	0.210	0.01580
10	4160 ± 30	89.5 ± 0.6	0.78	3.656	4.444	0.335	0.214	0.00676
11	4200 ± 30	89.9 ± 0.3	0.77	3.628	4.496	0.338	0.211	0.00651
12	4190 ± 30	89.9 ± 0.3	0.77	3.639	4.508	0.337	0.210	0.00400
13	4250 ± 30	89.5 ± 0.5	0.77	3.658	4.534	0.335	0.208	0.00332
14	4290 ± 100	89.4 ± 1.5	0.76	3.612	4.384	0.340	0.218	0.03680
15	4090 ± 50	89.5 ± 2.0	0.79	3.660	4.470	0.335	0.212	0.00843
16	4210 ± 60	89.7 ± 1.0	0.77	3.689	4.437	0.332	0.214	0.07426
17	4150 ± 30	89.3 ± 0.4	0.78	3.642	4.486	0.337	0.211	0.01444
18	4280 ± 20	89.2 ± 0.3	0.76	3.644	4.581	0.337	0.205	0.02985

FIXED PARAMETERS: $q = m_2/m_1 = 0.71$, mass ratio of the components; $T_1 = 5800$ K, temperature of the primary; $A_{s_{1,2}} = T_{s_{1,2}}/T_1 = 0.65$, spotted areas temperature coefficient; $f_1 = f_2 = 1.00$, non-synchronous rotation coefficients of the components; $\beta_1 = \beta_2 = 0.08$, gravity-darkening coefficients of the components; $u_1 = 0.66$, limb-darkening coefficient of the primary.
Note. No; data set number; $\theta_{1,2}$, spotted area angular dimensions; $\lambda_{1,2}$, spot longitude and $\varphi_{1,2}$, spot latitude (all in degrees); F_1, F_2, filling coefficients for critical Roche lobes of the primary and secondary; T_2, temperature of the secondary; i, orbital inclination (in degrees); u_2, limb-darkening coefficient of the secondary; Ω_1, Ω_2, dimensionless surface potentials of the primary and secondary; R_1, R_2, stellar polar radii in units of the distance between the component centres, and $\Sigma(O-C)^2$, final sum of squares of residuals between observed (LCO) and synthetic (LCC) light curves.

3 RESULTS

The light curve analysis is done in the frame work of the single and double spot models. Therefore, here we present only the solutions obtained under the double spot working hypothesis. In the programme these active regions are characterized by the temperature contrast of the spot with respect to the surrounding photosphere ($A_s = T_s/T_1$), by the angular dimension (radius) of the spot (θ) and by the longitude (λ) and latitude (φ) of the spot centre. The longitude (λ) is measured clockwise (as viewed from the direction of the $+Z$-axis) from the $+X$-axis (the line connecting the star centres) in the range $0°–360°$. The latitude (φ) is measured from $0°$ at the stellar equator (orbital plane) to $+90°$ at the "north" ($+Z$) pole and $-90°$ at the "south" ($-Z$) pole.

Table 2 presents the results of the light curve analysis in a "compressed" form. The table contains parameters of the system evaluated through the analysis of individual light curves, enumerated according to Table 1.

From Table 2, and from Figure 1(a) and Figure 2 it is evident that the synthetic light curves obtained by solving the inverse problem fit the observations very well. The system's basic parameters are approximately constant for the whole set of analysed light curves (see Figures 1(b), 1(c), 1(d)). This means that the changes in the light curve form can be almost completely explained by the changes in the position and size of the spotted areas for the entire observational period. A certain variability can be noticed in the temperature of the secondary, with the minimum value in light curve No. 15. A comparatively small depth of the secondary minimum of this light curve probably indicates a real phenomenon. The variations of the orbit's inclination are within the accuracy limits of this parameter's evaluation.

The change of active-region parameters over the analysed observational period can be presented on plots. Such a presentation is given in Figure 1 (right column). The spot migration in longitude during the analysed period is shown in Figure 1(e).

The spotted areas appear at high latitudes, near the polar regions (Figure 1(f)). In the case of the double spot model, the first larger spotted area is on the upper stellar hemisphere, near the polar region (latitudes $\varphi \sim (50°–86°)$. The second smaller spotted area is on the lower stellar hemisphere (latitudes $\varphi \sim (-5)°–(-70)°$).

The size of the spotted area can be an indicator of the system's activity. Based on the obtained results (Figure 1(g)) one can say that during 1973 the system showed a significant activity, while in 1974 the activity decreased.

Therefore, for light curve No. 10, obtained in late 1974, one finds minimum dimensions of the spotted areas. After this, there is a fast increase in the activity. In 1976 it reaches a lower level again, at which it remains with smaller changes till the end of 1980. It seems that then a new significant increase in the activity took place. Then the activity increases again. Unfortunately, the data available are not sufficiently dense in time to study the activity in more detail. A clear cyclicity in the system's activity is not noticeable.

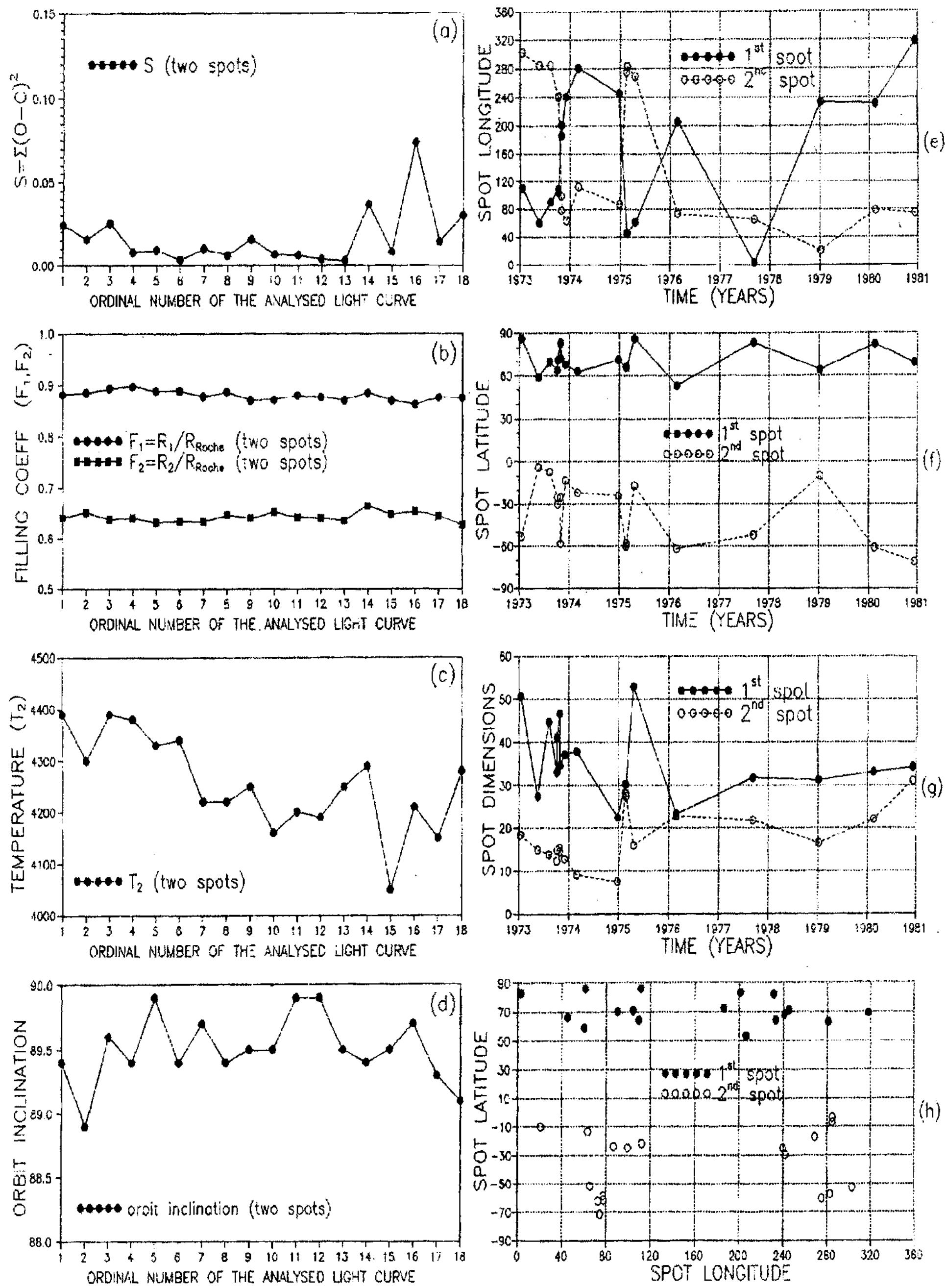

Figure 1 Solutions obtained by analysing the light curves of *SV Cam* within the framework of the Roche model with two spotted areas on the primary component: **Left**, quality of fitting (S) and basic system parameters ($F_{1,2}$, T_2, i) obtained by analysing the individual light curves; **Right**, spotted area parameters (λ, φ and θ) and (λ, φ) spot positions during the period 1973–1981.

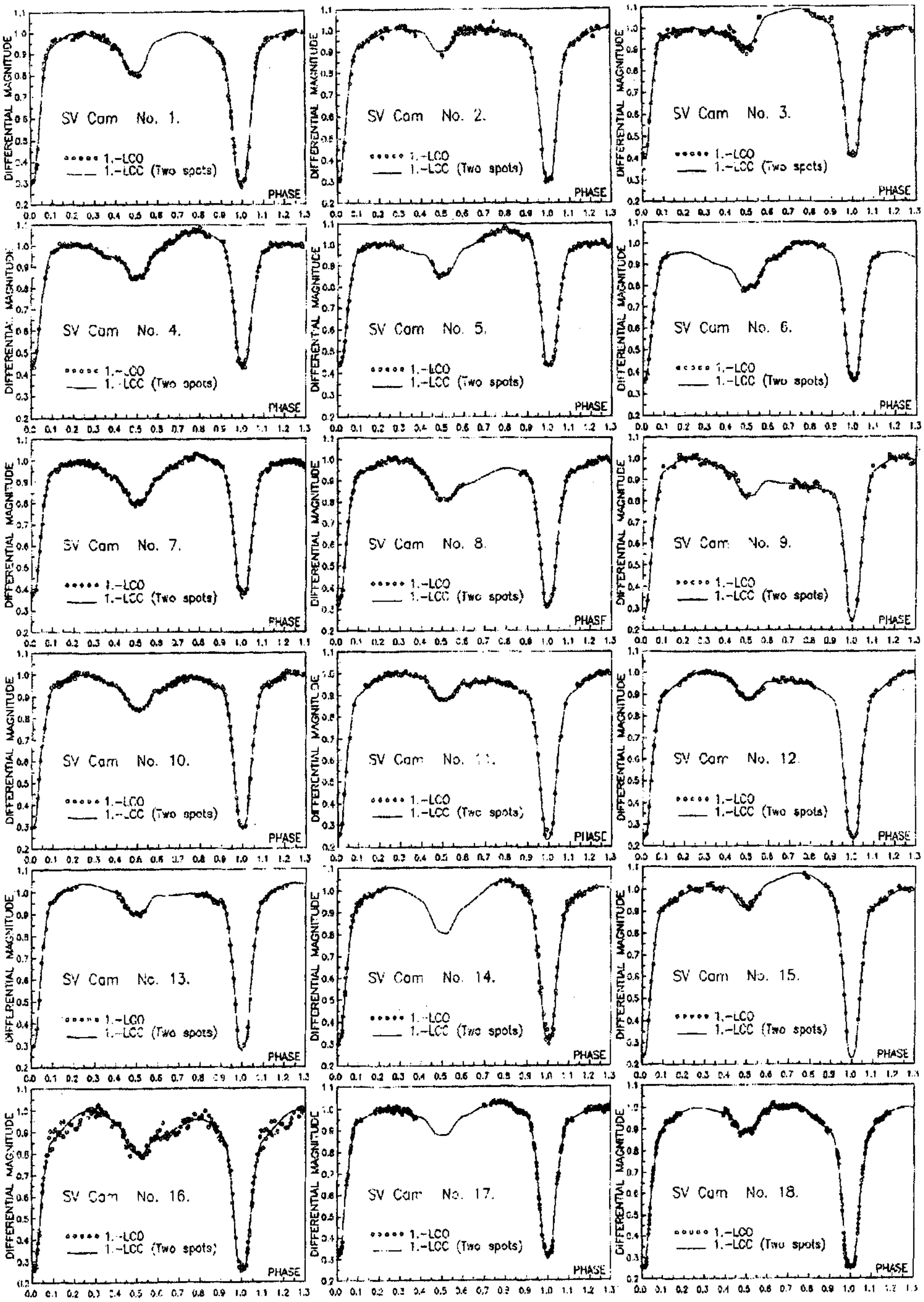

Figure 2 Observed (LCO) and final synthetic (LCC) light curves of *SV Cam* obtained by solving the inverse problem within the framework of the Roche model with two spotted areas on the primary component.

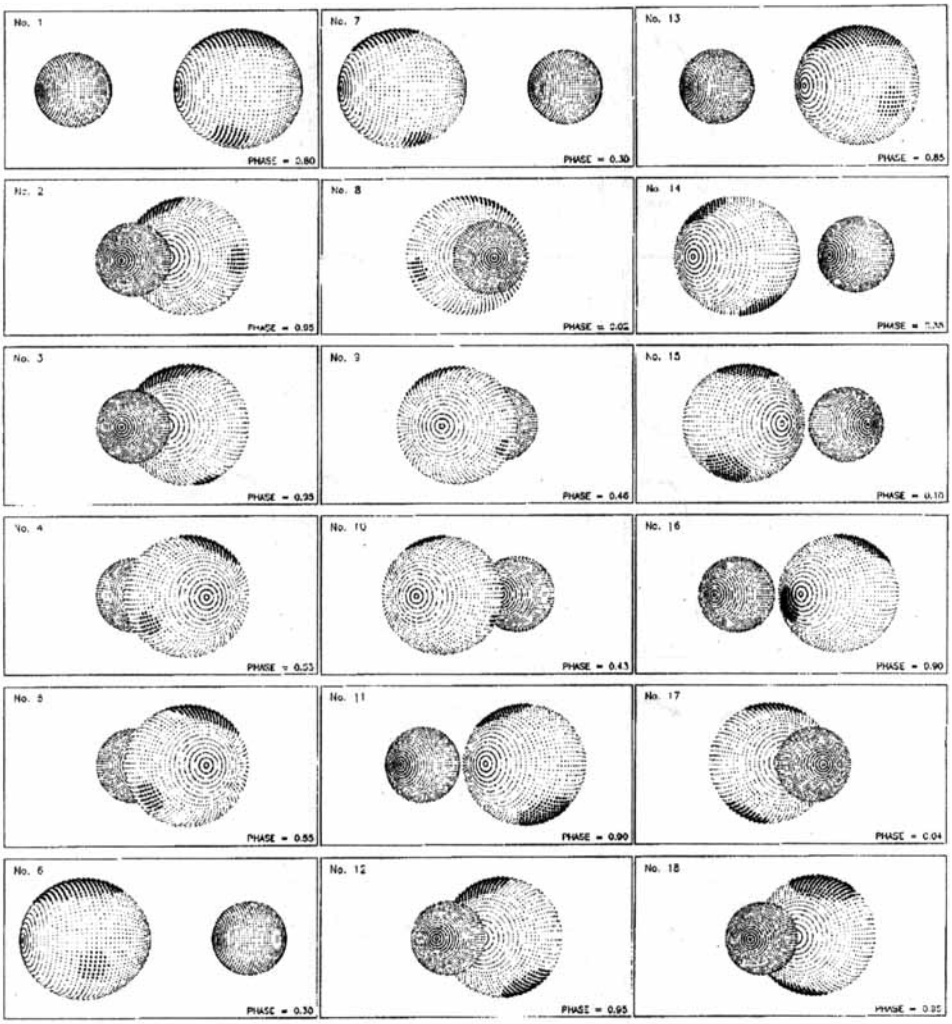

Figure 3 The view of the CB *SV Cam* at corresponding orbital phase with parameters obtained by solving the inverse problem.

During the analysed period, (λ, φ)-positions of the spotted area are grouped within active longitude and latitude sectors (Figure 1(h)). In the case of the double spot model the active longitude belts for the first spot in the intervals $\Delta\lambda \sim (45°–110°)$ and $\Delta\lambda \sim (200°–250°)$ are less prominent, but they are more prominent for the second spot in $\Delta\lambda \sim (60°–120°)$ and $\Delta\lambda \sim (240°–300°)$. The latitudes are concentrated within the sectors $\Delta\varphi \sim (50°–85°)$ (first spot) and $\Delta\varphi \sim ((-5)°–(-70)°)$ (second spot). Due to a selection effect it is possible that more extensive observational material would correct this result to some extent.

The obtained fit of the observed light curves (LCO) by the synthetic ones (LCC) following from the inverse problem solutions based on the single and double spot model, are shown in Figure 2. To easily follow the obtained solutions, the light curves are noted by ordinal numbers (No) according to those applied in Tables 1, 2.

Figure 3 shows the view of the system obtained from the parameters estimated by analysing the corresponding light curves. The enumeration of the figures corresponds to the ordinal number of the analysed light curves. The figures were made by using the programme (Djurašević, 1991). Thanks to such plots, one can see a view of a CB system at a noted orbital phase, chosen so that the spots are visible.

4 DISCUSSION AND CONCLUSIONS

Both presentations of the results (Table 2 and the corresponding figures) show that in the case of the Roche model with two spotted regions, the synthetic light curves obtained by solving the inverse problem fit the observations very well (almost within the measurement accuracy). The variations of the system's basic parameters among the different curves are insignificant for the period analysed. This means that the variations in the light curves can be explained by the change of the position and size of the spotted areas on the primary.

Appearing at high latitudes, the spotted areas cover a significant part of the stellar surface. Since the system's period is short ($P \sim 0\overset{d}{.}59$), the presence of spots at high latitudes (near the polar regions) can be explained by the dynamo mechanism for rapid rotators (Schüssler and Solanski, 1992).

References

Budding, E. (1973) *Astrophys. Space Sci.* **22**, 87.
Budding, E. (1977) *Astrophys. Space Sci.* **48**, 207.
Budding, E. and Najim, N. N. (1980) *Astrophys. Space Sci.* **72**, 369.
Budding, E. and Zeilik, M.(1987) *Astrophys. J.* **319**, 827.
Cellino, A., Scaltriti, F., and Busso, M. (1985) *Astron. Astrophys.* **144**, 315.
Díaz-Cordovés, J., Claret, A., and Giménez, A. (1995) *Astron. Astrophys. Suppl. Ser.* **110**, 329.
Djurašević, G. (1991) *Publ. Obs. Astron. Belgrade* **42**, 1.
Djurašević, G. (1992a) *Astrophys. Space Sci.* **196**, 241.
Djurašević, G. (1992b) *Astrophys. Space Sci.* **197**, 17.
Eaton, J. A. and Hall, D. S. (1979) *Astrophys. J.* **227**, 907.
Hall, D. S. (1976) In: W. S. Fitch (ed.), *Multiple Periodic Variable Stars*, Dordrecht, Reidel, p. 287.
Hilditch, R. W., Harland, D. M., and McLean, B. J. (1979) *Mon. Not. R. Astron. Soc.* **187**, 797.
Lucy, L. B. (1967) *Zs. f. Ap.* **65**, 89.
Marquardt, D. W. (1963) *J. Soc. Ind. Appl. Math.* **11**, No. 2, 431.
Osaki, Y. (1970) *Mon. Not. R. Astron. Soc.* **148**, 391.
Patkós, L. (1981) *Ap. Letters* **22**, 1.
Patkós, L. (1982) *Comm. Konkoly Obs.*, No. 80.
Schüssler, M. and Solanski, S. K. (1992) *Astron. Astrophys.* **264**, L13.
Torczon, V. (1991) *SIAM J. Optimization* **1**, No. 1, 123.
Wilson, R. E. and E. J. Devinney (1971) *Astrophys. J.* **166**, 605.
Zeilik, M., De Blasi, C. Rhodes, M., and Budding, E. (1988) *Astrophys. J.* **332**, 293.